ENGO 623 Inertial Surveying and INS/ GPS Integration

Project 4: Implementation of GPS / 3D RISS Integration using Loosely Coupled Integration

Instructor: Dr.Aboelmagd Noureldin

Student : Ranjeeth Kumar Siddakatte
UCID : 10119739

DEPARTMENT OF GEOMATICS ENGINEERING
UNIVERSITY OF CALGARY, ALBERTA, CANADA

List of Figures

Figure 1 Kingston road trajectory for different solutions....9
Figure 2 Position parameters comparison....10
Figure 3 Position error KF Open Loop....11
Figure 4 Velocity parameter comparison....11
Figure 5 Velocity errors....12
Figure 6 Azimuth error comparison....12
Figure 7 Zoomed in trajectory at two critical turns before tuning Qo....13
Figure 8 Zoomed in trajectory at turn 1 after tuning Qo....14
Figure 9 Zoomed in trajectory at turn 2 after tuning Qo....14
Figure 10 Effect large Q for whole trajectory - Xbow....14
Figure 11 Convergence plot of altitude error....15
Figure 12 Convergence plot of Angular velocity error....15
Figure 13 Closed loop KF v/s open loop KF at a sharp turn....16
Figure 14 Closed loop KF v/s open loop KF at increasing velocity....17
Figure 15 Track showing ten GPS outage introduced....17
Figure 16 Outage 1....18
Figure 17 Outage 2 and 3....18
Figure 18 Outage 4 and 6....19
Figure 19 Outage 8 and 5....19
Figure 20 Outage 7 and 9....20
Figure 21 Outage 10....20

List of Tables

Table 1 3D-RISS Mechanization Equations....6
Table 2 Dynamic error model....7

Acronyms and Symbols

3D	3-Dimensional
AR	AutoRegressive
ARMA	AutoRegressive Moving Average
ARW	Angle Random Walk
ENU	East North UP
GM	Gauss Markov
GPS	Global Positioning System
IMU	Inertial Measurement Unit
INS	Inertial Navigation System
ISA	Inertial Sensor Assembly
LLF	Local Level Frame
MEMS	Micro Electro Mechanical Systems
PVA	Position Velocity Attitude
RISS	Reduced Inertial Sensor System
RMSE	Root Mean Square Error
MSEE	Mean Square Estimation Error
x_k	k^{th} time epoch of x

1. ABSTRACT

This project explores the benefit of integrating two navigation solutions, INS and GPS, which have complementary characteristics. INS has better short term accuracy, with long term errors increase with time. On the other hand, the GPS has good long term accuracy. In this project, INS is integrated with GPS solution with a loosely coupled Kalman Filter (KF) approach. A 3D-RISS architecture is integrated in this approach is demonstrated to show the improvements in PVA accuracy, which is better than either INS or GPS standalone solution. This report also explores the performance improvement in a closed loop KF as compared to an open loop KF. Merits of integrated solution in GPS denied environments are also investigated by introducing GPS outages. Performance two types of IMUs, tactical and MEMS grade are analyzed, and efficient working of low cost MEMS in real time is demonstrated using road test experiment in a land vehicle. Advantages and limitations of the loosely coupled KF integration of RISS with GPS are also analyzed and discussed. This experiment uses a RISS involving a single-axis gyroscope and two-axis accelerometers together with a speed sensor to provide full navigation solution.

2. INTRODUCTION AND BACKGROUND

Positioning and navigation solution from a pure INS mechanization process is studied in literatures is not reliable over long time as the inherent sensor errors accumulate during the integration process [A. Noureldin, 2013]. Stochastic errors also contribute in considerable long term growth in errors, which makes INS not applicable for a standalone use. Also, most high-end inertial systems are all high cost. Global Positioning System (GPS) is used in most of the navigation systems as it is globally available and low cost. GPS requires signal from at least four satellites with good geometry [Kaplan, 2006]. Although GPS solution is reliable over long term when compared to INS, it suffers from short term errors and low output data rate. Availability of GPS satellite signal is not always guaranteed due to blockade from obstacles such buildings, overpasses, trees, etc. To overcome the standalone operating limitations of either GPS or INS, their complementary performance characteristics can be exploited to integrate two systems, such that they augment each other.

Kalman Filter is widely used to integrate INS and GPS [Umar et al, 2008]. Many types of integration are studied in literatures, loose coupling, tight coupling, and ultra-light coupling [Gebre

2007]. In this project KF integration with loose coupling is investigated. In loose coupling, INS and GPS operate individually to provide separate navigation solution. The position and velocity difference of two solutions is fed to an optimal filter, in this case the KF. The KF estimates the INS errors based upon the error models. The estimated errors are removed from INS solution to provide an integrated solution, which will be better than the standalone solution of either of the systems. The KF used here is independent of the KF used inside GPS.

As discussed earlier, high end inertial systems are costly and bulky. Research is going on towards developing light weight, economical, and simpler inertial systems with the development of MEMS technology. Also, use of full IMU mechanization will be too erroneous to due complex interlinked errors between many inertial sensors [A. Noureldin 2013]. Hence it is wise to use reduced number of sensors to provide navigation solution so that the time dependent errors will be minimized to a large extent.

The goal of this project is to investigate the methods and analyze the results of fusing RISS and GPS with a loosely coupled Kalman Filter approach to provide a 3D navigation solution. Dynamic error models and Measurement models for KF are developed in Section 3. Implementation, investigation, and analysis of results are demonstrated in Section 4. Conclusion of the research is presented in Section 5, followed by the list of referred literatures in Section 6.

3. THEORY AND METHOD

3D-RISS mechanization discussed in this project is demonstrated for land vehicular movement application to obtain a 3-D navigation solution. Since a land vehicle moves mostly in horizontal plane, it makes use of 4 sensors. A gyroscope is placed in z direction of the body. It measures the angular velocity in z direction, used to calculate the Azimuth angle. Two accelerometers are used, one mounted in forwards direction (y-axis), and the other mounted in transverse axis (x-axis). An odometer is used, which is mounted in forward axis, used to measure forward velocity.

The process of obtaining an integrated RISS/ GPS solution involves following steps.

1. Obtain the 3D-RISS mechanization equations.
2. Obtain the dynamic error model of mechanization equations
3. Obtain the models for Loosely Coupled RISS/ GPS Integration
    a. System Model
    b. Measurement Model
4. Kalman Filter

a. Open Loop

b. Closed Loop

3.1. 3D-RISS Mechanization Equations

A set of simplified mechanization equation are written in Table 1.

Table 1 3D-RISS Mechanization Equations

$p = sin^{-1}\left(\frac{f_y - a_{od}}{g}\right)$	p = Pitch angle, f_y= Y axis Accelerometer data, a_{od} = forward acceleration, g = gravity
$r = -sin^{-1}\left(\frac{f_x + v_{od}\omega_z}{g}\right)$	r = Roll angle, f_x = X axis Accelerometer data v_{od} = forward velocity, ω_z = Z axis gyro data
$\dot{A} = -\left(\omega_z - \omega^e sin\varphi - \frac{v_e tan\varphi}{(R_N + h)}\right)$	A = Azimuth angle, ω^e = Earth rotation rate R_N = Normal radius
$\begin{pmatrix} v_e \\ v_n \\ v_u \end{pmatrix} = \begin{pmatrix} v_{od}\sin(A)cos(p) \\ v_{od}\cos(A)cos(p) \\ v_{od}sin(p) \end{pmatrix}$	v_e = East velocity v_n = North velocity v_u = Up velocity
$\begin{pmatrix} \dot{\varphi} \\ \dot{\lambda} \\ \dot{h} \end{pmatrix} = \begin{pmatrix} 0 & \frac{1}{R_M + h} & 0 \\ \frac{1}{(R_N + h)cos\varphi} & 0 & 0 \\ 0 & 0 & 1 \end{pmatrix} \begin{pmatrix} ve \\ vn \\ vu \end{pmatrix}$	φ = Latitude λ = Longitude h = Altitude

3.2. Dynamic Error Model of Mechanization Equations

The error state vector, δx_k proposed for this experiment includes position errors (δφ, δλ, δh), velocity errors (δv_e, δv_n, δv_u), azimuth error (δA), sensor errors (δa_{od}, $\delta \omega_z$). They are derived from the mechanization equations by linearizing through Taylor series expansion method and ignoring higher order terms [A. Noureldin, 2013]. A simplified set of error state equations are written in Table 2 ignoring the relatively smaller terms for some states. However it should be noted that consider those terms will improve the performance.

$\delta x_k = [\delta\varphi, \delta\lambda, \delta h, \delta v_e, \delta v_n, \delta v_u, \delta A, \delta a_{od}, \delta \omega_z]_k$;

Table 2 Dynamic error model

$\begin{pmatrix}\dot{\delta\varphi}\\ \dot{\delta\lambda}\\ \dot{\delta h}\end{pmatrix}=\begin{pmatrix}0 & \frac{1}{R_M+h} & 0\\ \frac{1}{(R_N+h)cos\varphi} & 0 & 0\\ 0 & 0 & 1\end{pmatrix}\begin{pmatrix}\delta ve\\ \delta vn\\ \delta vu\end{pmatrix}$
$\begin{pmatrix}\dot{\delta v_e}\\ \dot{\delta v_n}\\ \dot{\delta v_u}\end{pmatrix}=\begin{pmatrix}a_{od}cosAcosp & sinAcosp & 0\\ -a_{od}sinAcosp & cosAcosp & 0\\ 0 & sinp & 0\end{pmatrix}\begin{pmatrix}\delta A\\ \delta a_{od}\\ \delta\omega_z\end{pmatrix}$
$\begin{pmatrix}\dot{\delta A}\\ \dot{\delta a_{od}}\\ \dot{\delta\omega_z}\end{pmatrix}=\begin{pmatrix}0 & 0 & -1\\ 0 & -\gamma_{od} & 0\\ 0 & 0 & -\beta_{\omega_z}\end{pmatrix}\begin{pmatrix}\delta A\\ \delta a_{od}\\ \delta\omega_z\end{pmatrix}$

3.3. Discrete time KF models for Loosely Coupled RISS/ GPS Integration

3.3.1. System Model

System model of discrete time KF is given by [A. Noureldin, Spring 2013]

$$\delta x_k = (I + F\Delta t)\delta x_{k-1} + G\Delta t w_{k-1}$$

I is the Identity matrix. F is the dynamic coefficient matrix corresponding to the error state vector δx_k. It is written from Table 2 as follows,

$$F=\begin{pmatrix}O_{3X3} & F1 & O_{3X3}\\ O_{3X3} & O_{3X3} & F2\\ O_{3X3} & O_{3X3} & F3\end{pmatrix},\quad F1=\begin{pmatrix}0 & \frac{1}{R_M+h} & 0\\ \frac{1}{(R_N+h)cos\varphi} & 0 & 0\\ 0 & 0 & 1\end{pmatrix},$$

$$F2=\begin{pmatrix}a_{od}cosAcosp & sinAcosp & 0\\ -a_{od}sinAcosp & cosAcosp & 0\\ 0 & sinp & 0\end{pmatrix},\ F3=\begin{pmatrix}0 & 0 & -1\\ 0 & -\gamma_{od} & 0\\ 0 & 0 & -\beta_{\omega_z}\end{pmatrix},\ O_{3X3}=\begin{pmatrix}0 & 0 & 0\\ 0 & 0 & 0\\ 0 & 0 & 0\end{pmatrix}$$

Product Gw_{k-1} is the process noise, which is the noise associated with the states due to the mechanization model.

$Gw_{k-1} = [\sigma_{\varphi}, \sigma_{\lambda}, \sigma_{h}, \sigma_{ve}, \sigma_{vn}, \sigma_{vu}, \sigma_{A}, \sigma_{od}\sqrt{2\beta_{od}}, \sigma_{wz}\sqrt{2\gamma_{\omega z}}]^{T}$;

3.3.2. Measurement Model

The measurement model of a discrete time KF is expressed as

$\delta z_k = H_k \delta z_k + n_k$

δz_k is the measurement vector, the different between position parameters and velocity parameters predicted by INS and the corresponding values measured by the GPS.

$$\delta z_k = \begin{bmatrix} \varphi_{INS} - \varphi_{GPS} \\ \lambda_{INS} - \lambda_{GPS} \\ h_{INS} - h_{GPS} \\ ve_{INS} - ve_{GPS} \\ vn_{INS} - vn_{GPS} \\ vu_{INS} - vu_{GPS} \end{bmatrix}$$

H_k is the design matris giving ideal noiseless relationship between the observation vector and the state vector. For the present project, it is a 6 X 9 matrix as shown below. n_k is the measurement noise which is assumed to be a white noise, uncorrelated with process noise w_k.

$$H_k = \begin{bmatrix} 1 & 0 & 0 & 0 & 0 & 0 & 0 & 0 & 0 \\ 0 & 1 & 0 & 0 & 0 & 0 & 0 & 0 & 0 \\ 0 & 0 & 1 & 0 & 0 & 0 & 0 & 0 & 0 \\ 0 & 0 & 0 & 1 & 0 & 0 & 0 & 0 & 0 \\ 0 & 0 & 0 & 0 & 1 & 0 & 0 & 0 & 0 \\ 0 & 0 & 0 & 0 & 0 & 1 & 0 & 0 & 0 \end{bmatrix}$$

3.4. Kalman Filter

KF which is used as an optimal estimator for error states also outputs real time statistical data related to estimation accuracy in the form of error co-variance matrix P_k, which is very useful for quantitative error analysis [Brown, 2012].

$P_k = E[(x_k - \hat{x}_k)(x_k - \hat{x}_k)^T]$; $\hat{x}_k$ is the estimated error state at time epoch *k*

The diagonal elements of P matrix can be analyzed in real time for convergence towards minimal mean square estimation error (MSEE).

KF is experimented with both open loop and closed loop architectures [A. Noureldin, 2013] and performance is compared in the following section.

4. ANALYSIS AND RESULTS

Loosely coupled KF integration of 3D-RISS solution is implemented in MATLAB. Real road test data are collected from following IMUs: IMU300CC-100, a MEMS IMU from Crossbow and a tactical grade IMU from Honeywell, IMU-G2-H58. They will be referred as Xbow and Novatel throughout this literature. Reference trajectory used in this experiment is the one from Novatel-SPAN unit integrated with Honeywell-IMU-G2-H58. Initially, an open loop filter is used for analyzing the significance of integration.

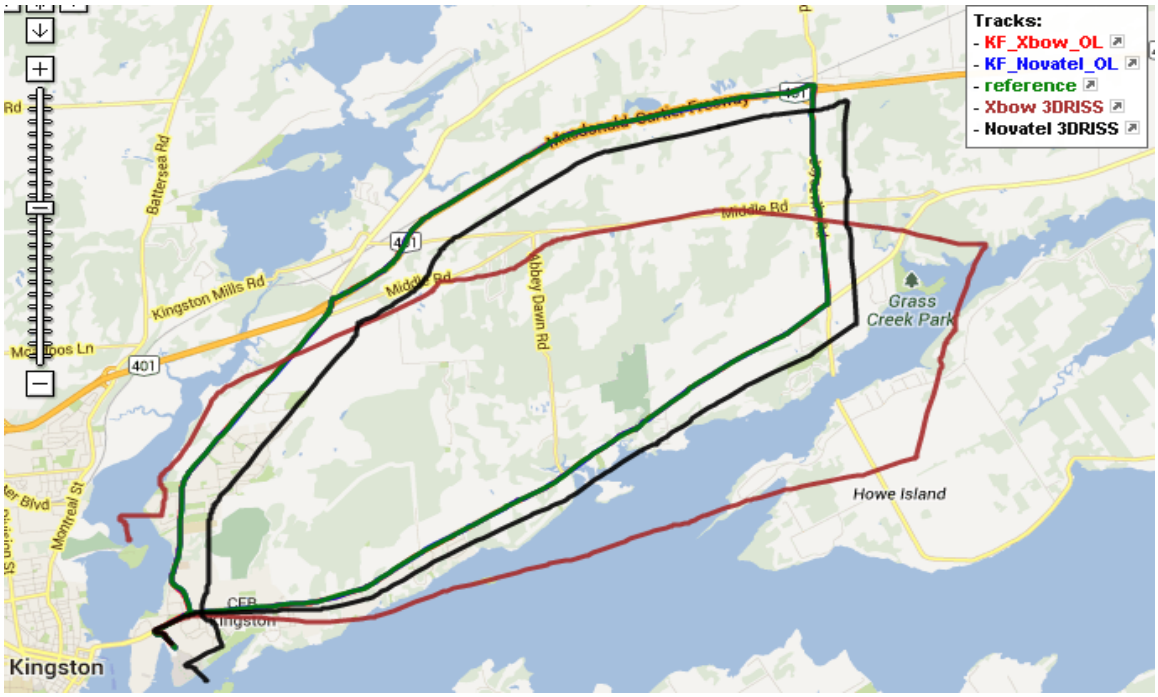

Figure 1 Kingston road trajectory for different solutions

4.1. KF Output compared against pure 3D-RISS Output

Figure 1 shows the road trajectory obtained from different solutions. It can be seen clearly that neither the Novatel 3D-RISS solution nor the Xbow-3D RISS solution overlaps with the reference. The integrated solution from both Xbow and Novatel IMUs overlap with the solution, which signifies the importance of integrating two solutions capitalizing their inverse accuracy characteristics with respect to time.

4.1.1. Position Parameters

Figure 2 shows the comparison of position parameters with respect to the reference. It can be verified that for both types of sensors, KF integration yields a good results.

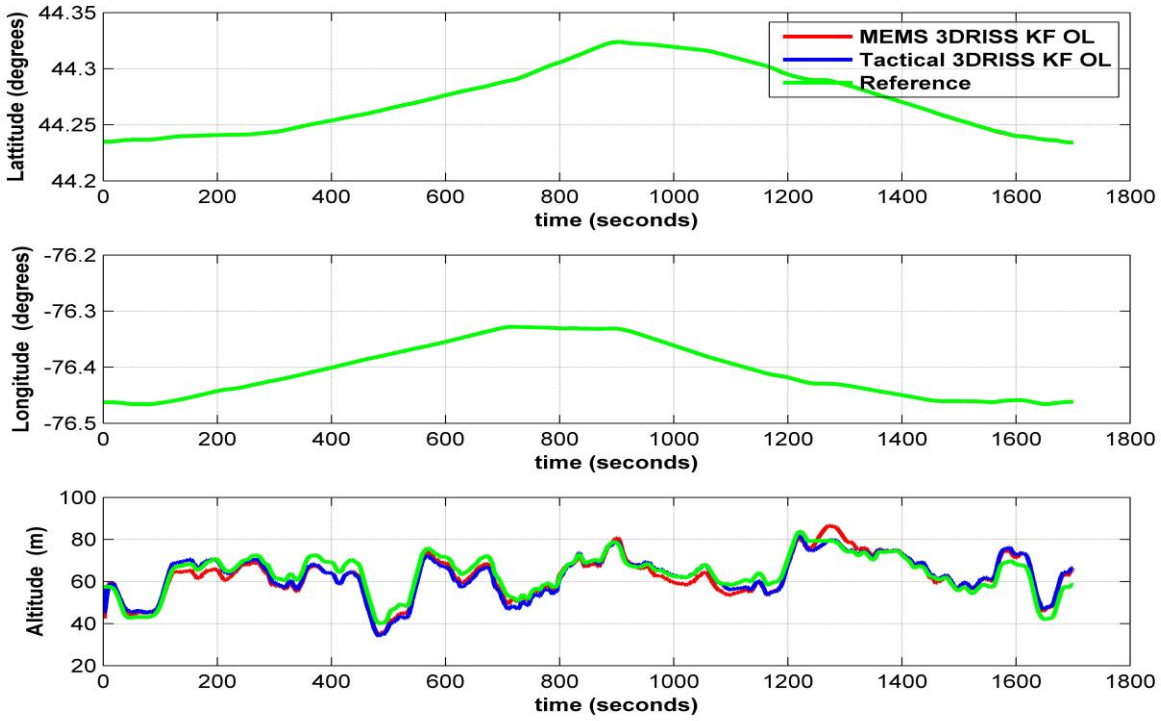

Figure 2 Position parameters comparison

Figure 3 shows the position errors, which indicates position errors for MEMS grade are higher when compared to the tactical grade. It is an expected result as the process noise of MEMS mechanization is higher than that of tactical grade. It should be noted that these errors did no grow with time. This is effect of KF integration which removed INS long term errors by coupling it with GPS solution. Also, it is observed that the height error of MEMS grade pure KF-3DRISS is limited within -25 meters, whereas for a pure 3D-RISS, it was around -200 meters at the end of the trajectory. This effect is not shown to clearly distinguish height error of tactical grade with that of MEMS grade.

4.1.2. Velocity Parameters

Figure 4 is the plot of comparing velocity parameters of KF integrated solution compared with the reference. Both east and north velocities overlap with reference. Up velocity is showing small variations, but it was observed that it is significantly less compared that of a pure 3D-RISS solution. These small variations are due to that fact that since pitch and roll errors are not included in error state vector, these are not corrected. Up velocity is directly proportional to sine of the pitch velocity. Pitch depends on X-axis accelerometer. By including these two states in error model,

performance can be improved. Variation in Up velocity results altitude error as in Figure 3. Velocity errors are indicated in Figure 5

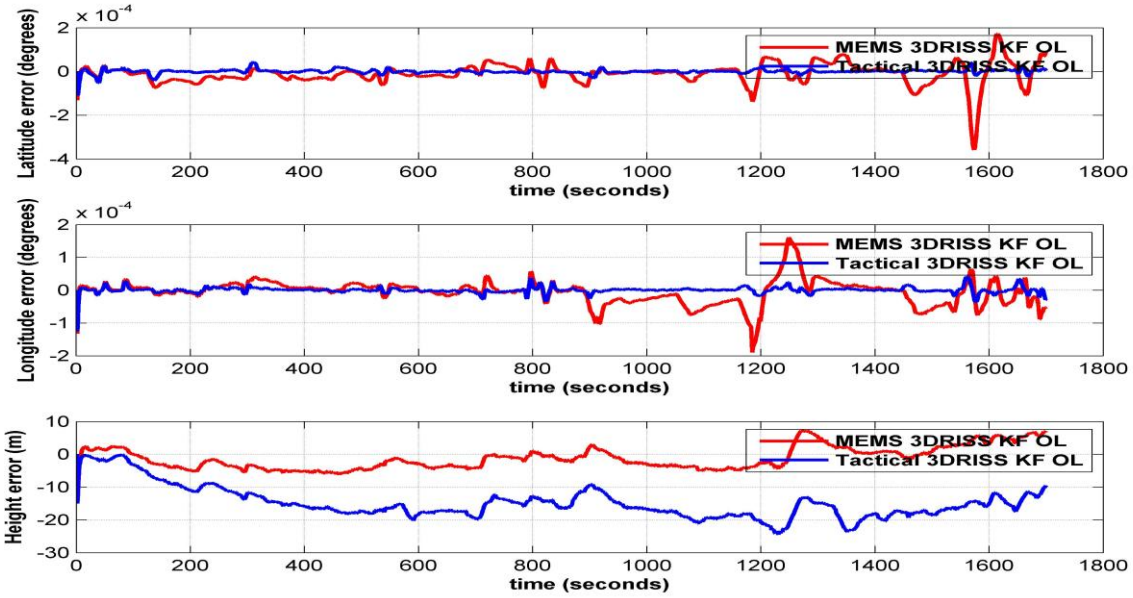

Figure 3 Position error KF Open Loop

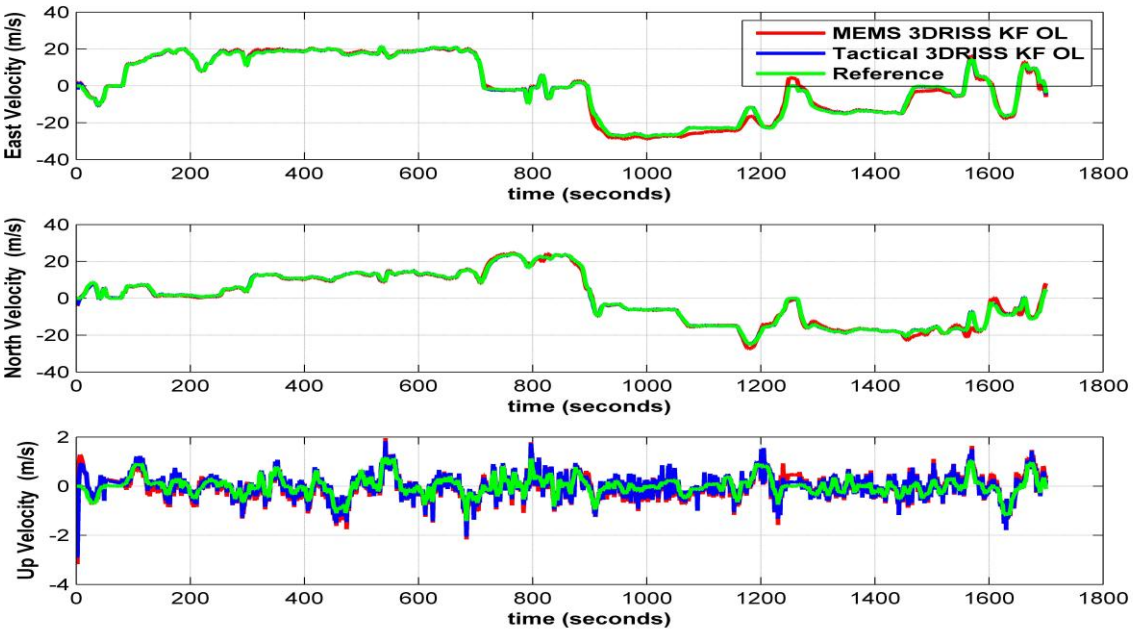

Figure 4 Velocity parameter comparison

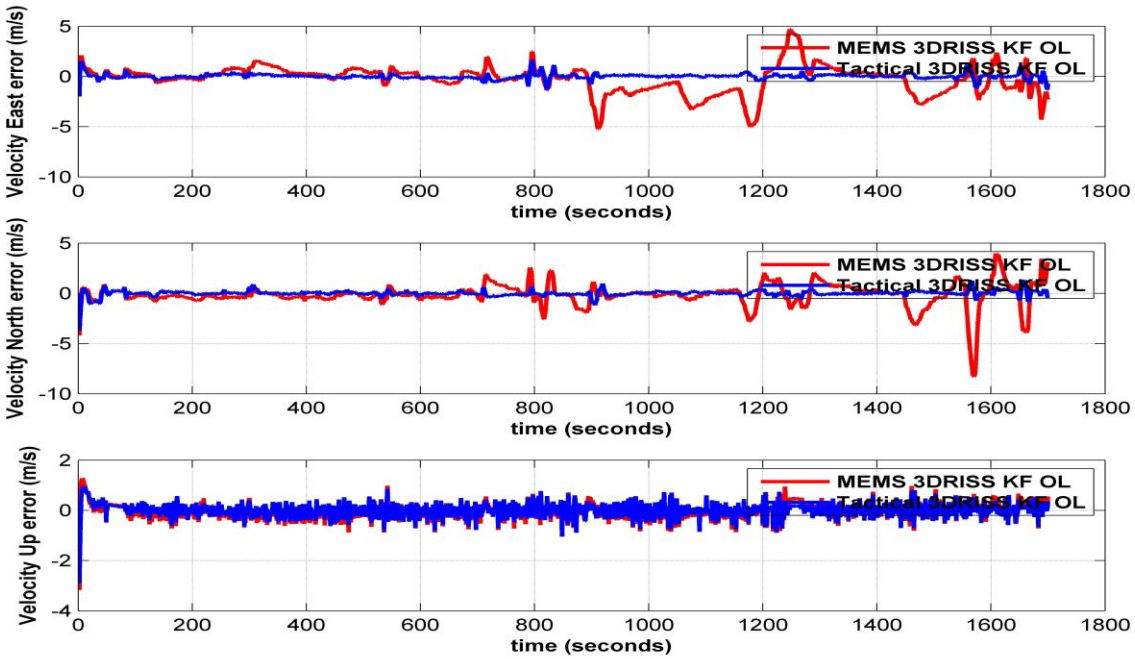

Figure 5 Velocity errors

4.1.3. Azimuth

Figure 6 shows the azimuth error plot for different solutions. As expected, azimuth error of a pure 3DRISS for MEMS grade (Xbow) is growing with time. It corrected by the KF integration process, which is shown in red line. Similarly, the azimuth error of integrated solution is better than the pure 3D-RISS mechanization for tactical grade as well.

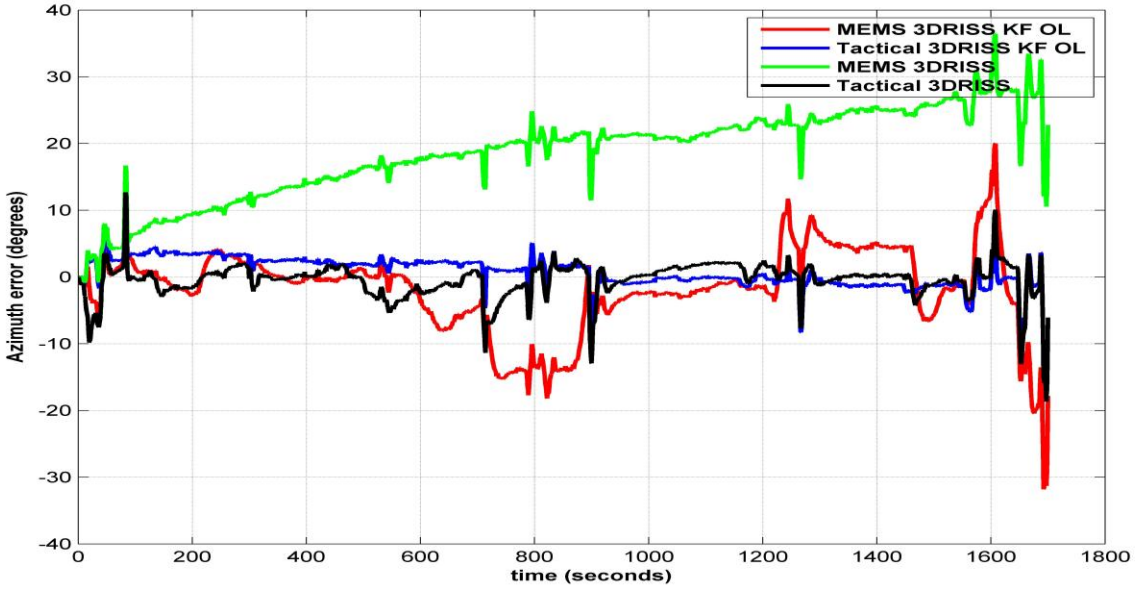

Figure 6 Azimuth error comparison

Further investigation can be done by zooming in the trajectory at the regions of critical importance.

4.2. Importance of tuning the KF initial states

It is very important to tune the initial states of KF. Tuning is done with prior experience with the system for a given dynamics of the vehicle. The initial error state vector x_0, the process noise covariance matrix Q_0, the estimation error covariance matrix P_0 all needs to be tuned initially. The measurement noise covariance matrix R is computed from standard deviations of GPS measurement parameters.

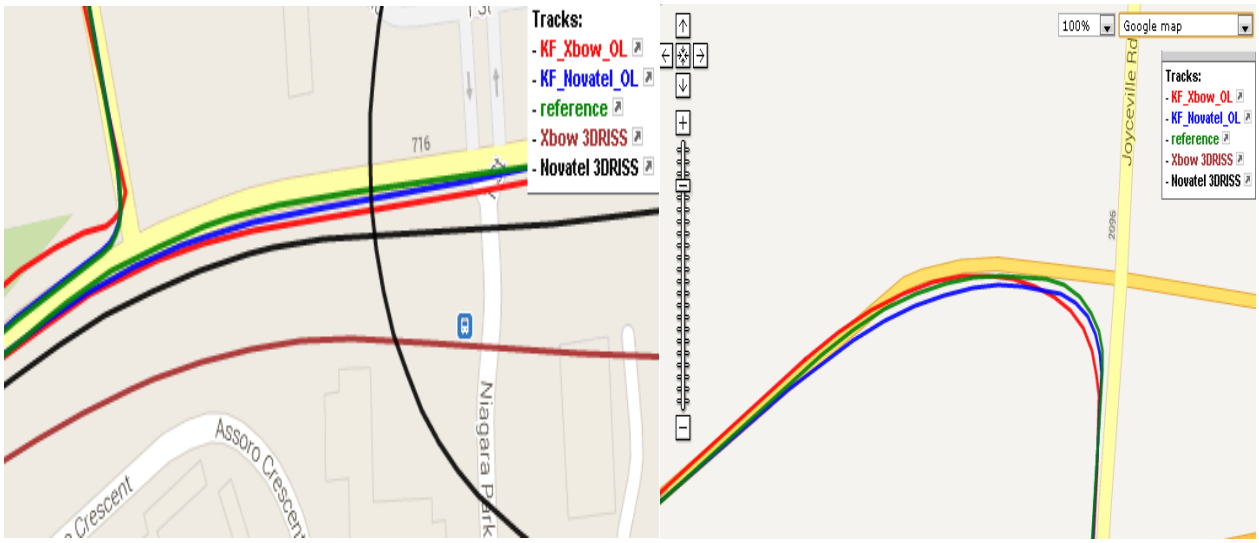

Figure 7 Zoomed in trajectory at two critical turns before tuning Qo

Figure 7 shows the zoomed in trajectory at two turns before tuning. It can be seen that the KF solution is deviating away the reference. This is due to the facts that Q_0 was set very low value, indication the process noise is less erroneous. Hence the KF gain, K matrix is reduced, giving less importance to GPS measurements. Or in other words, KF relied on INS more. Figure 8 and Figure 9 show the improvement in KF solution after tuning the Q_o set for relatively higher value. Now KF relied more on GPS than INS and gave a better result. Integrated solution position parameters are overlapping with the reference. Figure 10 shows the effect of a large R matrix values and medium Q matrix values for whole trajectory, demonstrated for Xbow IMU data. In this case, KF relied less on GPS measurements and moderately more on INS measurements. Hence the trajectory deviated from reference, tending to move towards the pure 3DRISS trajectory along with the time.

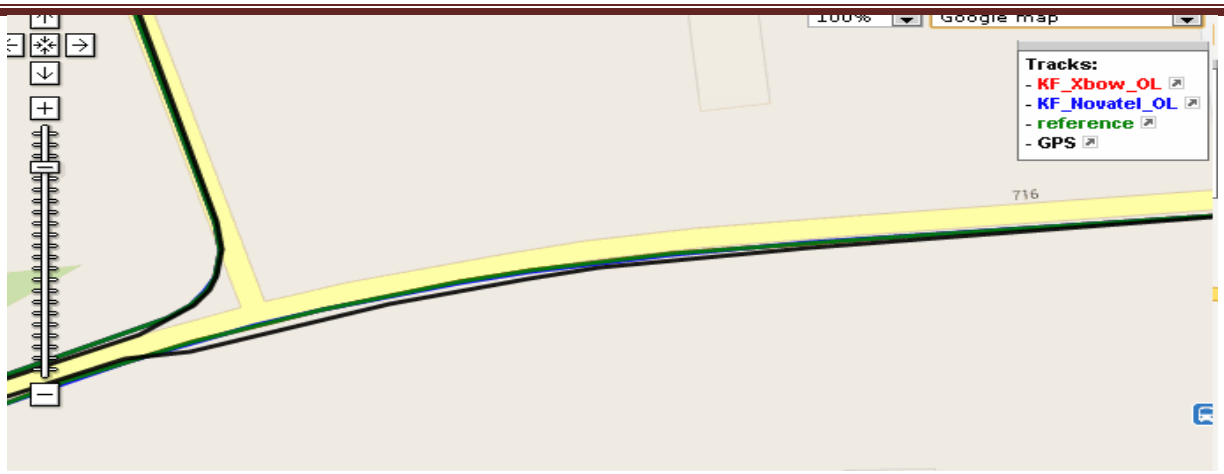

Figure 8 Zoomed in trajectory at turn 1 after tuning Qo

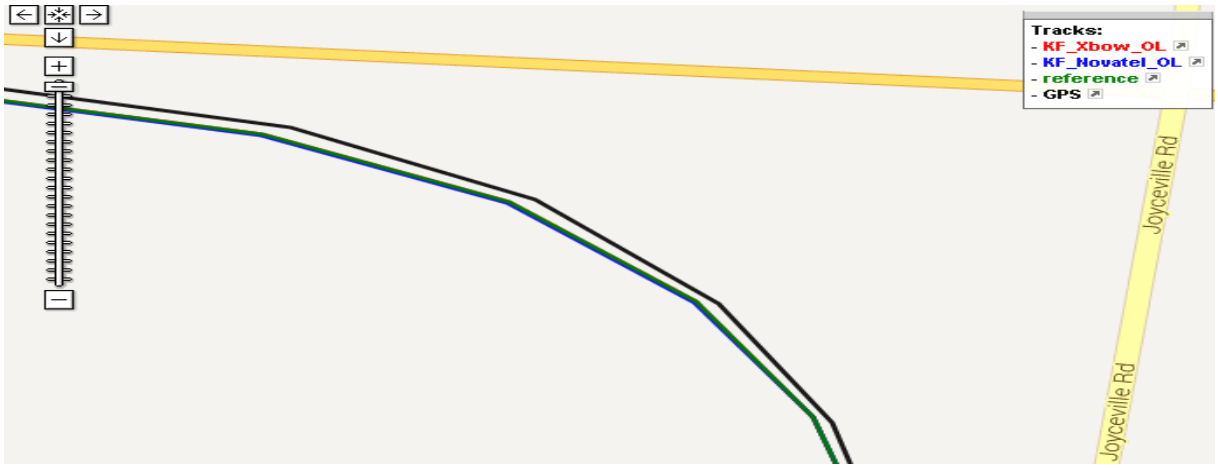

Figure 9 Zoomed in trajectory at turn 2 after tuning Qo

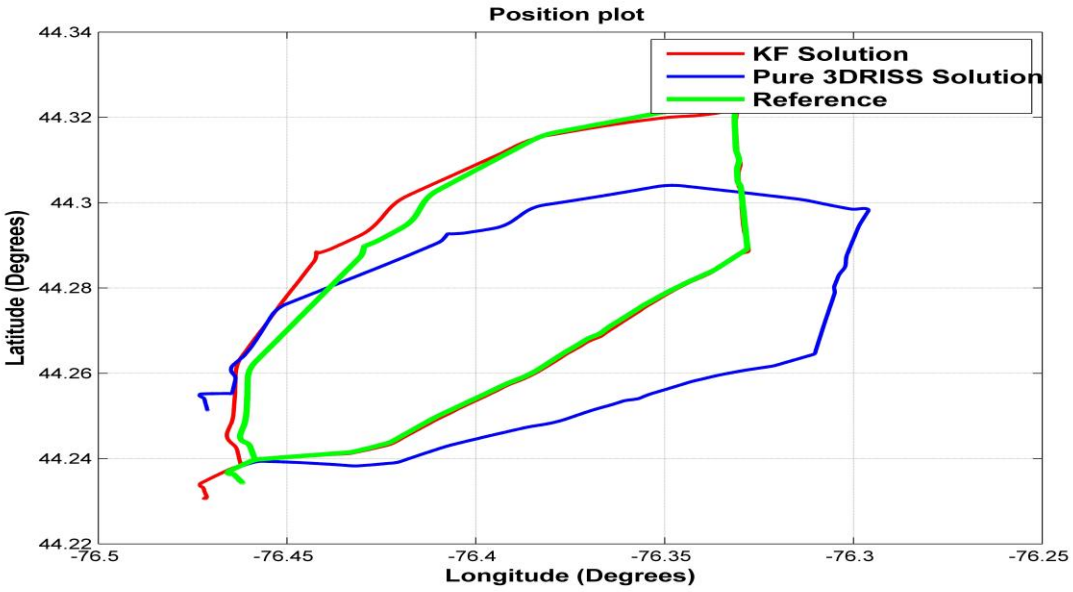

Figure 10 Effect large Q for whole trajectory - Xbow

4.3. Comparing with GPS data

It can also be observed in Figure 9 that the GPS trajectory (shown in black) is poor than the integrated solution. This confirms that the integrated KF achieves better result than the measurement input itself.

4.4. Convergence and P matrix elements

As discussed earlier, the diagonal elements of estimation error covariance matrix, P act as a real time metric to determine the accuracy of integrated solution. Integration process works towards minimizing the MSEE of the states of the model.

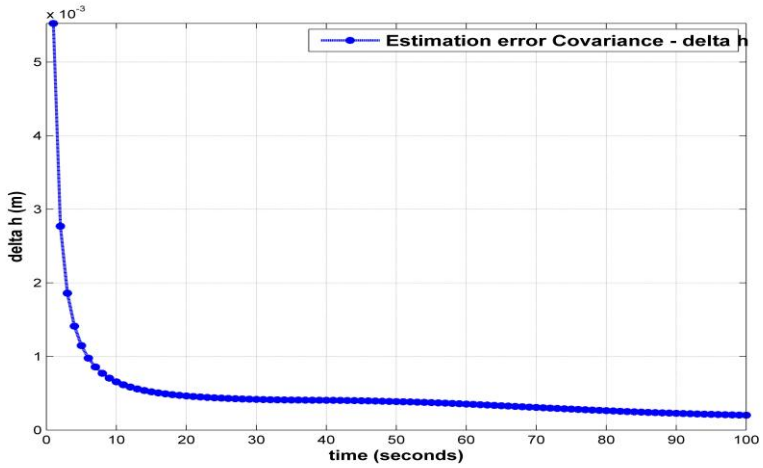

Figure 11 Convergence plot of altitude error

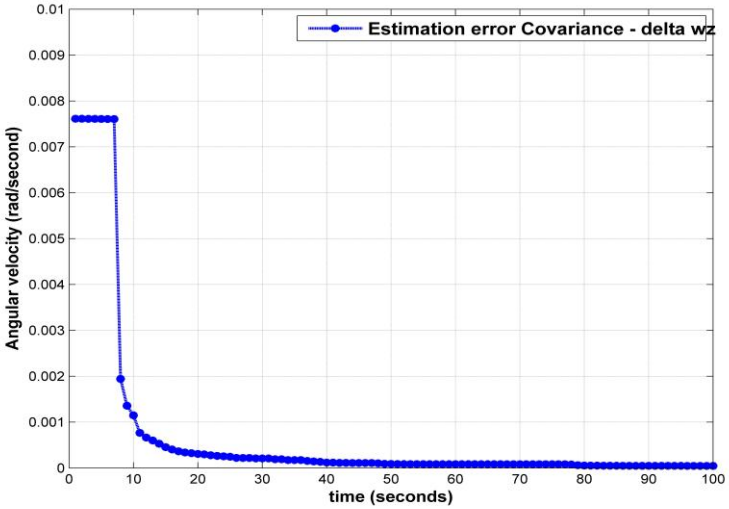

Figure 12 Convergence plot of Angular velocity error

Figure 11 and Figure 12 show the convergence plot for estimates of error states corresponding to altitude and angular velocity respectively, shown for Novatel data KF integration. These are derived from the diagonal elements corresponding to altitude error and angular velocity error, from the estimate error covariance matrix P. Similar convergence performance is achieved for other state vector elements by proper settings of initial P. It is observed that setting relatively large value for P_0 results in slow convergence (high valued/randomly changing P elements). Similarly, setting P_0 elements to very small values resulted in slow convergence. Convergence decides how fast accurate result can be obtained from KF.

4.5. Closed Loop Loosely Coupled KF

Closed loop KF is compared with the performance of an open loop KF suing data from Xbow IMU. It is observed that the performance of these two modes of integration can be distinguished by keeping moderate Q_0 value as it was not possible to clearly isolate the trajectories at low Q_0. Figure 13 shows the plot of trajectory of and open loop (blue) and closed loop (red) filters at a sharp turn (rate of change of Azimuth and Gyro data is more). Since the error states, including the δA and $\delta\omega_z$ are fed back for correcting INS measurements, the position parameters at the sharp turn, are overlapping with the reference. Since the feedback is absent in open loop, change in error estimates are not reflected, hence the deviation in position parameter.

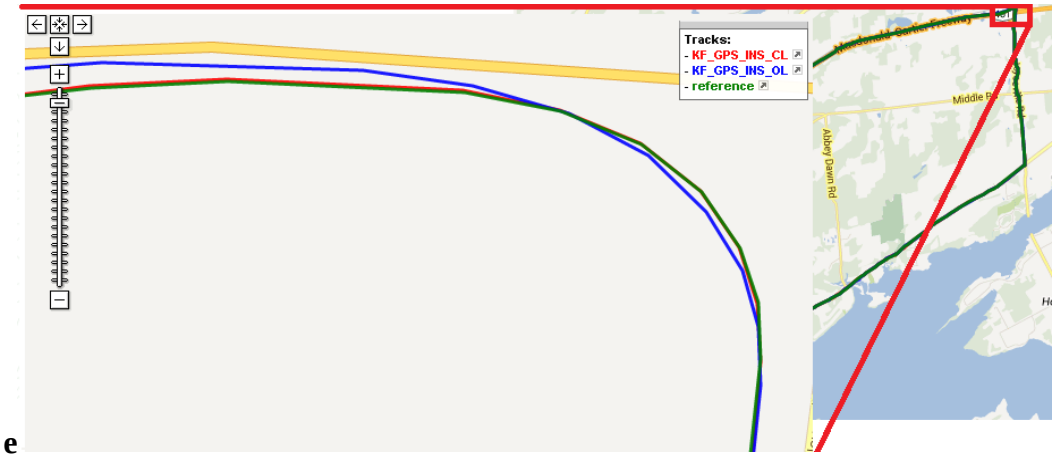

e

Figure 13 Closed loop KF v/s open loop KF at a sharp turn

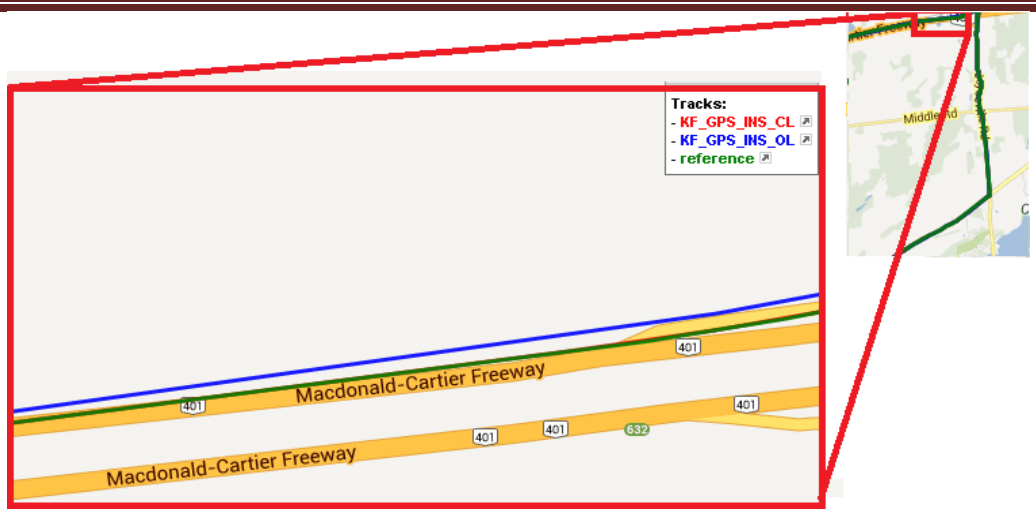

Figure 14 Closed loop KF v/s open loop KF at increasing velocity

Figure 14 shows another area in trajectory where there is an increasing speed. At this point, the east velocity is increased (in negative direction). Velocity errors are fed back for corrections, position parameters are accurate than that of open loop filter. It has to be noted from Table 2 that, position error is direction proportional to velocity errors, which is in turn proportional to Azimuth error.

4.6. Introducing Outages

The closed loop and open loop configurations are tested by introducing artificial GPS outages at intervals where there are changes in states, such as increasing east velocity, sharp turns, gradual changes in velocities, down hills etc.

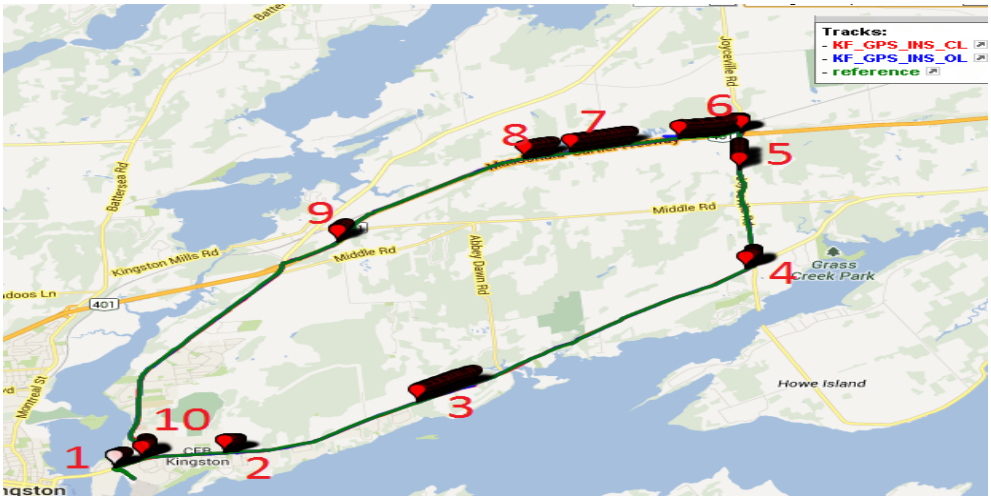

Figure 15 Track showing ten GPS outage introduced

Figure 15 shows the GPS visualizer graph of 10 outages at various locations. Outages are indicated by red pointers Duration of the outages is not fixed, it is varied (10 to 20 seconds) to test the performance of the loop to the best possible extent.

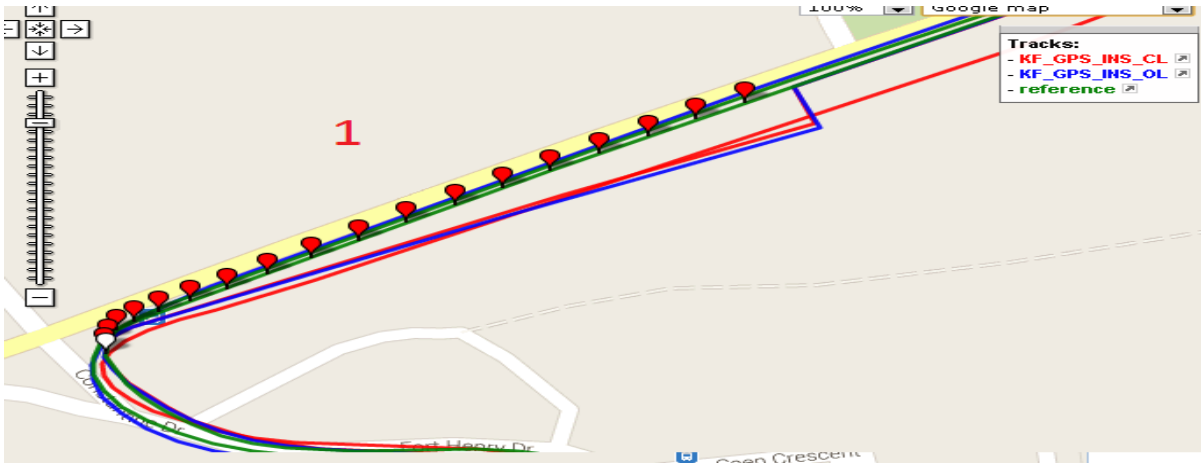

Figure 16 Outage 1

Figure 1 shows the first outage, it can be seen that at this sharp turn (large azimuth change) open loop output has deviated to small extent compared to closed loop. This is due to the fact the closed loop has just started working when the outage was introduced. Hence, a small improvement in performance.

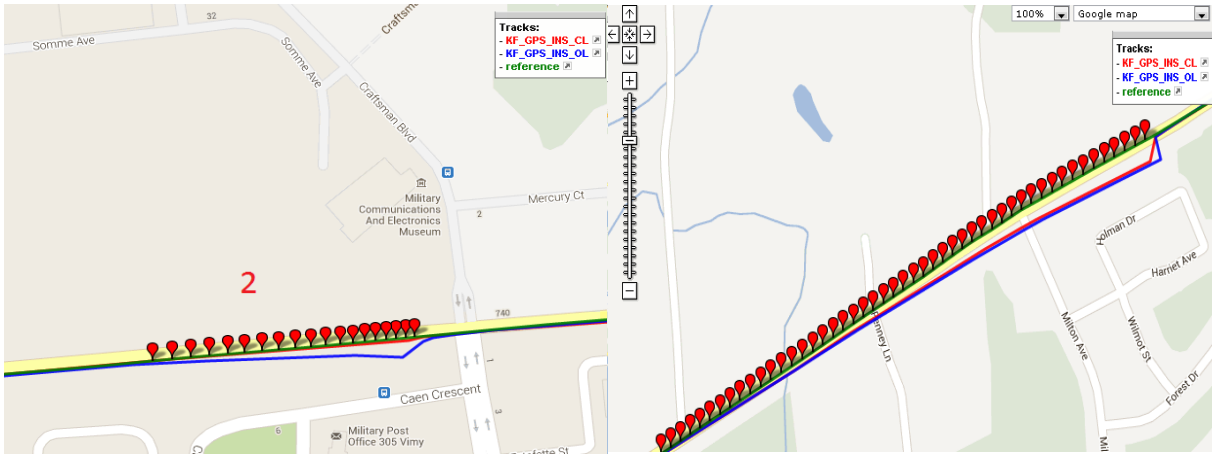

Figure 17 Outage 2 and 3

Figure 17 shows the outage 2. Here since the east and north velocity has picked up slowly, whose error states are fed back to the INS, hence trajectory is overlapping with the reference although the open loop output has deviated to a large extent due to outage. Similar result is seen for outage 3, but still better than the open loop solution.

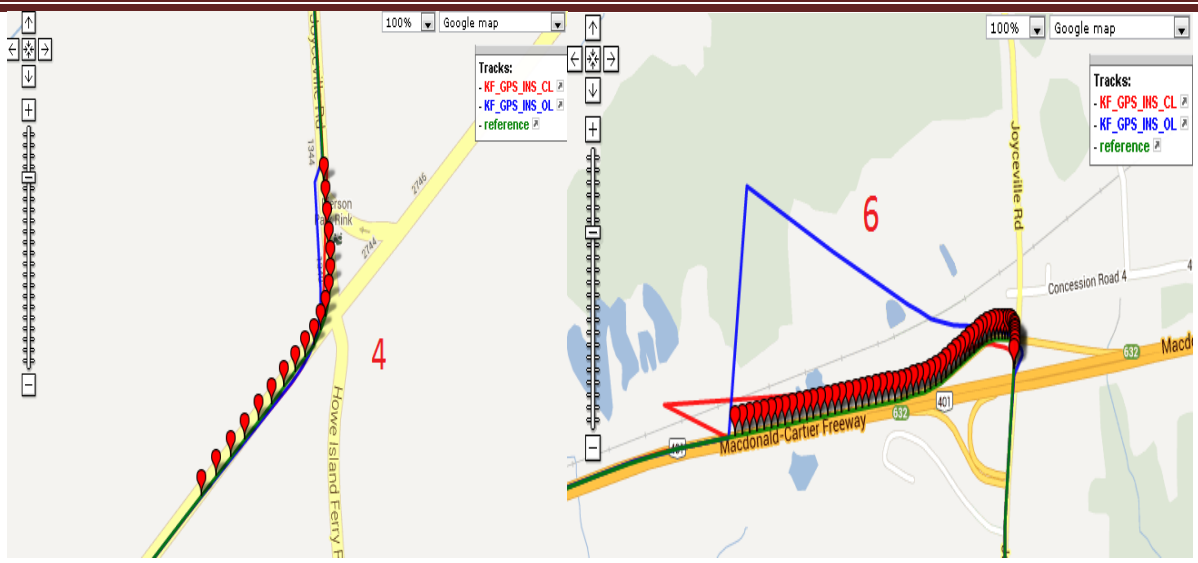

Figure 18 Outage 4 and 6

Figure 18 shows a sharp turns, where solution of open loop has deviated to a large extent, whereas open loop solution is intact due to change in azimuth error state is corrected.

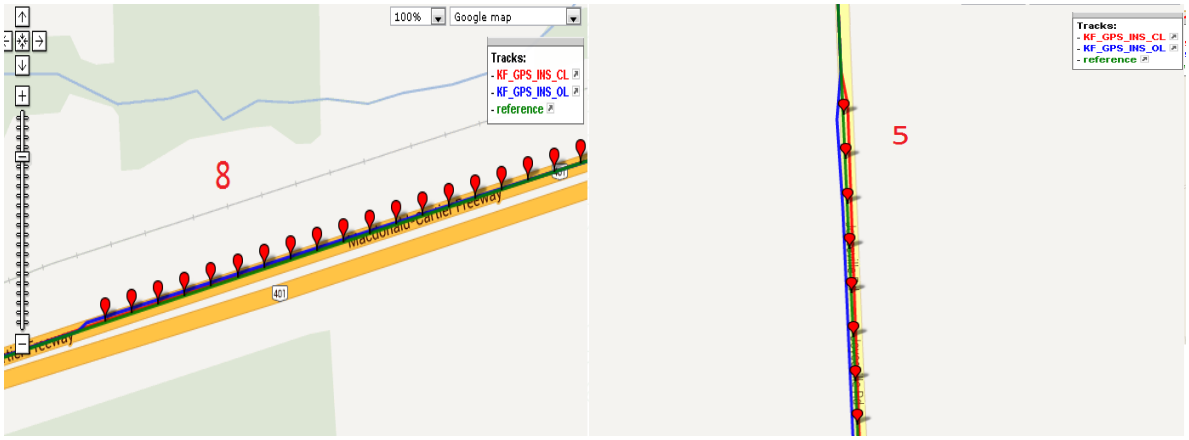

Figure 19 Outage 8 and 5

Figure 19 shows the outage 8 and 5, one is horizontal heading and other one in vertical heading. Deviation from closed loop solution is almost similar in both the case. This is due to the effect of east and north velocities respectively. In both cases, velocity is almost constant, which contributes minimal deviation of open loop solution since there is not drastic change in velocity. Also other contributing factor such as azimuth error is also relatively very small. Figure 20 shows the outage 7, and outage 9, in both case open loop is affected by increasing change in velocities. Outage 10 towards end of the trajectory, shown in Figure 21 shows large deviation in open loop solution due to multiple reasons 1) Large change in azimuth 2) Sudden variation in velocity 3) time dependent inherent errors. It can be seen that open loop solution has been deviated away from the reference at the beginning of outage.

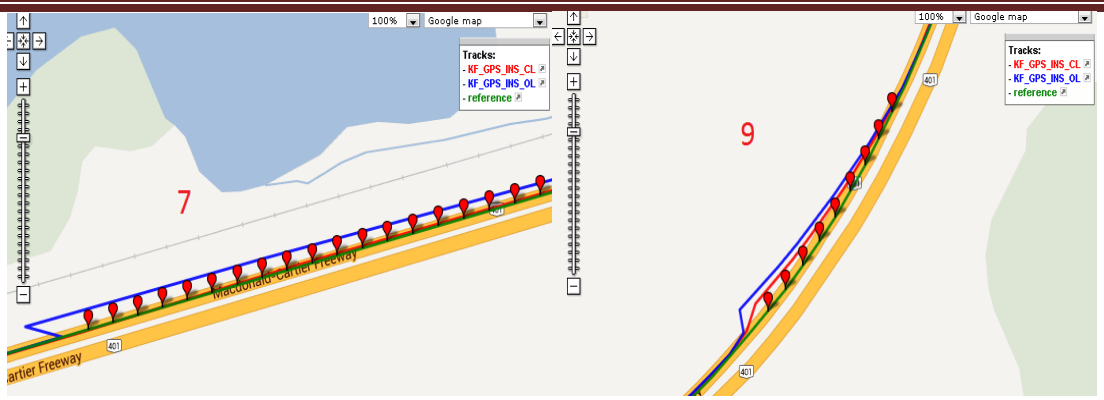

Figure 20 Outage 7 and 9

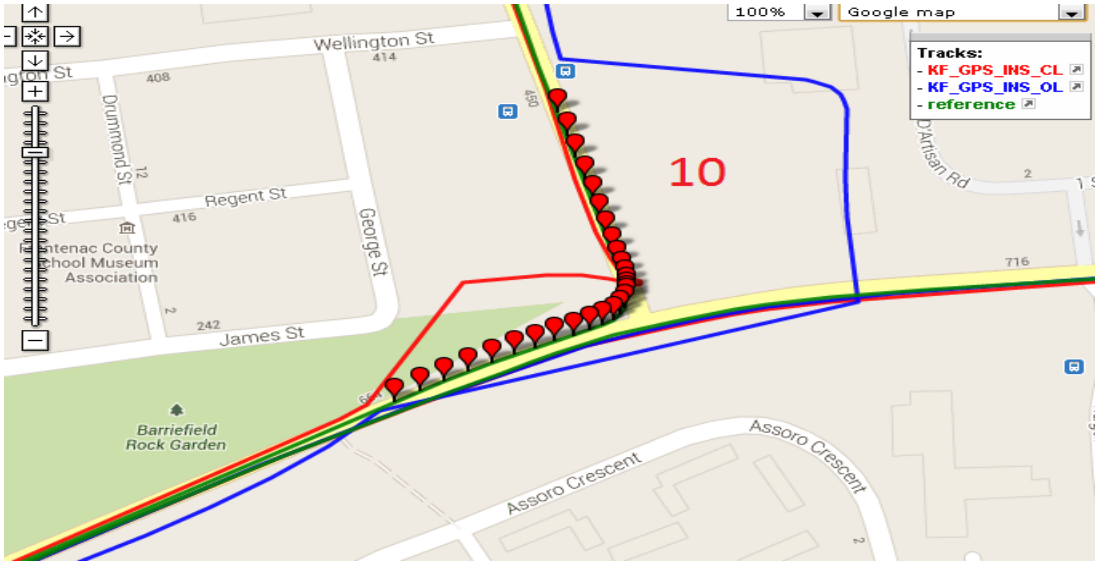

Figure 21 Outage 10

5. CONCLUSION

The experiment of integrating two navigation solution through loosely coupled Kalman filter resulted in following conclusions.

- The integrated solution is better than either of the solutions, stand-alone INS or GPS could provide
- Initializing the states of KF to a proper value is very essential to have a good performance throughout the trajectory for a given dynamics.
- The real time accuracy of the estimated states can be verified by the estimate error covariance matrix, an output from KF.
- Closed loop KF performs better than the open loop during GPS outages as the error states are fed back for correction.

- Exiting limitations (deviation from reference) can be corrected by adding additional states to KF and also by considering all the terms in error model.

6. REFERENCES

1 Noureldin, A. (Spring 2013), Inertial Navigation and INS/GPS Integration course, ENGO 623 Course Notes, Department of Geomatics engineering, University of Calgary, Canada

2 Aboelmagd Noureldin, Tashfeen B. Karamat A. Jacques Georgy, (2013), Fundamentals of Inertial Navigation, Satellite-based Positioning and their Integration. ISBN: 978-3-642-30465-1 (Print) 978-3-642-30466-8 (Online)

3 U. Iqbal, A. F. Okou, and A. Noureldin, "An Integrated Reduced Inertial Sensor System—RISS/GPS for Land Vehicle," in *Proceedings of IEEE/ION Position, Location and Navigation Symposium (PLANS '08)*, pp. 1014–1021, Monterey, California, USA, May 2008.

4 http://www.gpsvisualizer.com/tutorials/tracks.html, last accessed on June 14, 2013.

5 Matthew Cossaboom, Javques Georgy, Tashfeen B. Karamat, and A. Noureldin , "Augmented Kalman Filter andMapMatching for 3D RISS/GPS Integration for Land Vehicles", in *Hindawi Publishing Corporation International Journal of Navigation and Observation*, Volume 2012, Article ID 567807

6 MATLAB R2012a, Feb 2012, Version 7.14.0739, Help toolbox.

7. U. Iqbal, Tashfeen B. Karamat, A. F. Okou, and A. Noureldin , "Experimental Results on an Integrated GPS and Multisensor Systemfor Land Vehicle Positioning", in *Hindawi Publishing Corporation International Journal of Navigation and Observation*, Volume 2009, Article ID 765010

8. E.D Kaplan, *Understanding GPS: Principles and application 2nd ed.*, Boston MA: Artech House 2006

9. An Integrated Reduced Inertial Sensor System -RISS / GPS for Land Vehicle, Umar Iqbal, Aime Francis Okou, and Aboelmagd Noureldin, *Position, Location and Navigation Symposium*, 2008 IEEE/ION

10. Gebre-Egziabher D (2007) What is the difference between 'loose', 'tight' and 'ultra-tight' and 'deep' integration strategies for INS and GNSS. InsideGNSS

11. R.G. Brown, P.Y.C. Hwang, Introduction to Random Signals and Applied Kalman Filtering with MATLAB Exercises, 4e, John Wiley & Sons, Inc., 2012